ELSEVIER

Ceramics International 25 (1999) 517–522

CERAMICS INTERNATIONAL

Analysis of the microstructural evolution in hydroxyapatite ceramics by electrical characterisation

M.A. Fanovich*, M.S. Castro, J.M. Porto López

Instituto de Investigaciones en Ciencia y Tecnología de Materiales (INTEMA), CONICET Universidad Nacional de Mar del Plata, J.B.Justo 4302, (7600) Mar del Plata, Argentina

Received 23 July 1997; accepted 9 September 1997

Abstract

The aim of this work is to determine the effect of lithium or magnesium addition on the microstructure of hydroxyapatite ceramics sintered at 1200°C. The samples were characterised by density measurements, scanning electron microscopy (SEM), X-ray diffraction (XRD) and Vickers microhardness. Dielectric properties, dc-conductivity and microhardness were related to the microstructures developed by the sintered materials. Furthermore, significant effects due to the presence of Li^+ or Mg^{+2} in these ceramics were established.

1. Introduction

Hydroxyapatite [$Ca_{10}(PO_4)_6(OH)_2$] (HA) is the main inorganic phase of the calcified tissues of vertebrates. Different synthetic forms of HA are chemically similar to the inorganic phase in the natural bone. As a material for osseous implants, hydroxyapatite shows excellent properties because of its biocompatibility and capacity of regeneration of calcified tissues. However, due to its fragility, dense HA is used only in implants which are not submitted to high mechanical stresses. It has been determined that mechanical properties of HA may be improved by microstructural control through sintering processes [1]. Furthermore, those high densities and controlled microstructures can be obtained through modifications in the sintering process by the presence of several additives [2].

Goto and co-workers [3] studied the sintering mechanism of HA with different concentrations of lithium phosphate, and reported the formation of a liquid phase at 1010°C. The low temperature at which the liquid is formed could permit the development of coating techniques with this material. However, it should be kept in mind that Li^+ additions in the sintering of HA could result in biomaterials displaying a certain toxicity. The information about the effects of Li^+ in living organisms is scarce; however, it is known that because of its small size, Li^+ ions can pass through biological membranes and reach control sites. From this point of view, a possible interference of Li^+ with Na^+, K^+, Ca^{2+} or Mg^{2+} metabolism is possible, although toxicity depends on various factors, among which concentration is particularly important [4,5].

On the other hand, Okazaki et al. [6] studied the effect of Mg^{2+} on the crystallinity of HA, establishing that it inhibits the crystallisation of the apatitic structure. It is known that the substitution of Mg^{2+} by Ca^{2+} in synthetic hydroxyapatites is very limited, because of the appreciable difference between their ionic radii. Also, it has been reported that the crystallinity of the substituted material is reduced and its solubility increased, respect to those of Mg-free HA.

For a complete microstructural characterisation of sintered materials containing additives, it is necessary to know the distribution of these additives in the structure. Taking into account their different mobilities in the bulk material, the analysis of the electrical behaviour is a valuable tool for the description of this distribution [7]. Electrical measurements are a rapid and non-destructive method for determining physical properties such as porosity, permeability, etc. Dielectric constant measurement is also a standard method of characterisation of solids. In this way, not only electrical characteristics, but also physical and structural characteristics may be evaluated [8].

* Corresponding author.

0272-8842/99/$ - see front matter
PII: S0272-8842(97)00087-4

In this work, samples of non-stoichiometric HA with low concentrations of Mg^{+2} or Li^{+} sintered at 1200°C were analysed. Measurements of dissipation factor, dielectric constant and dc-conductivity vs temperature and time were correlated with the microstructures, phase composition, densification and microhardness of the samples.

2. Materials and methods

A commercial HA (Sigma Chem.Co.), with a molar ratio Ca/P = 1.51, was used in this study. The powder was precalcined 1 h at 500°C, and afterwards $LiNO_3$ or $Mg(NO_3)_2$ were added by impregnation with aqueous solutions to incipient wetting. Table 1 shows the final compositions of impregnated samples. The obtained powders were uniaxially compacted at room temperature, without binder. The sintering process was done at atmospheric pressure, for 1 h at 1200°C. Archimedes method was used for the measurement of densities. Fracture surfaces of the samples, with and without chemical etching (50% HCl; 20 s at room temperature) were observed by SEM. XRD analysis was performed with a Philips diffractometer, using CuK_α radiation and Ni filter, at 40 kV and 20 mA. The electrical measurements were performed on silver-coated samples. DC-conductivities were measured with a Keithley 614 electrometer and a Phitronics source (0-60 V, 0-2 A), applying a voltage of 10V in the range 20–400°C. Determinations of dielectric constant and dissipation factor were carried out with a Hewlett-Packard 4284A impedance analyser at frequencies between 100 Hz and 1 MHz. The samples, included in epoxy resin, were mirror-polished with diamond paste (1 μm) for the Vickers indentation tests. The microhardness values were determined under 300, 400 and 500 gf loadings.

3. Results and discussion

XRD analysis showed that in all samples, the main phases present were HA and β-tricalcium phosphate [β-$Ca_3(PO_4)_2$, β-TCP]. (Fig. 1(a) and (b)) From these diffractograms, it was observed that Mg^{2+} addition results in modifications of intensity and angular position of β-TCP peaks [2]. The presence of poorly crystalline MgO was also detected. In addition, a diminution in the β-TCP content was also observed in the samples with Li^{+}.

The densities of samples are given in Table 2. These values show that low Li^{+} concentrations enhance HA densification. This behaviour is attributed to the formation of a liquid phase during thermal treatment, which facilitates material transport. In the samples with Mg^{2+}, the densification degree increases slightly only when Mg^{2+} concentration is 1% Mg^{2+}. At higher Mg^{2+} contents, lower densities were observed.

The microstructures of the samples containing Li^{+} (Fig. 2) show a significative grain growth of HA, favoured by the formation of liquid phase at the sintering temperature. We suppose that, this liquid phase consists of lithium and calcium phosphates from the dissolution of β-TCP; then, the concentration of β-TCP in the crystalline phase is reduced, resulting in a more homogeneous microstructure.

Fig. 3 shows the dc-conductivity vs 1/T curves for samples with Li^{+}. The addition of 0.2% Li^{+} produces a

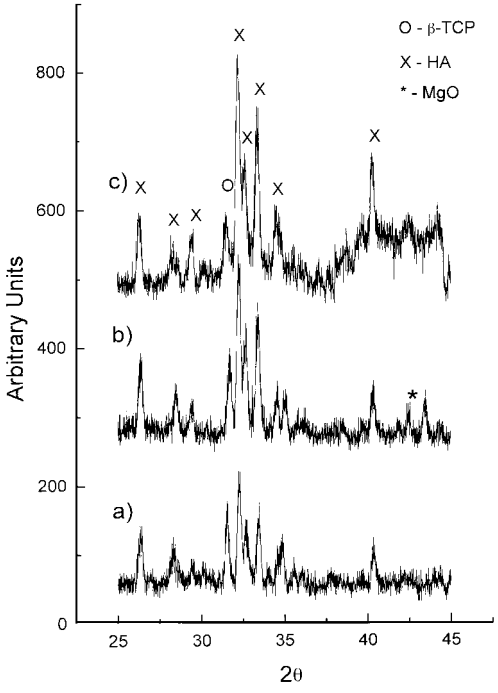

Fig. 1. XRD diffractograms of HA samples: (a) A; (b) F; (c) C.

Table 1
Additives incorporated to HA (% by weight)

Sample	% of Li^{+}	% of Mg^{+2}
A	–	–
B	0.2	–
C	0.4	–
D	–	1.0
E	–	3.0
F	–	5.0

Table 2
Densities of samples sintered with lithium or magnesium

Sample	Density ($g\,cm^{-3}$)
A	2.7
B	3.03
C	2.99
D	2.83
E	2.67
F	2.62

slight decrease in conductivity which is correlated with a diminution in the β-TCP [10] content. To explain this decrease in the conductivity, it must be considered that in sample A, the available carriers are H^+ in HA [9] and oxygen vacancies in β-TCP; for this reason, a decrease in β-TCP concentration lowers the conductivity. To confirm this hypothesis, the conductivity of pure β-TCP was measured, resulting in a higher conductivity than that of sample A, which contains HA and β-TCP. On the other hand, the conductivity of the sample C was an order of magnitude larger than the rest of the samples in the series. This higher conductivity could be caused by the presence of an appreciable amount of vitreous phase, which facilitates ionic mobility, and by the presence of Li^+, which could act as an new additional carrier.

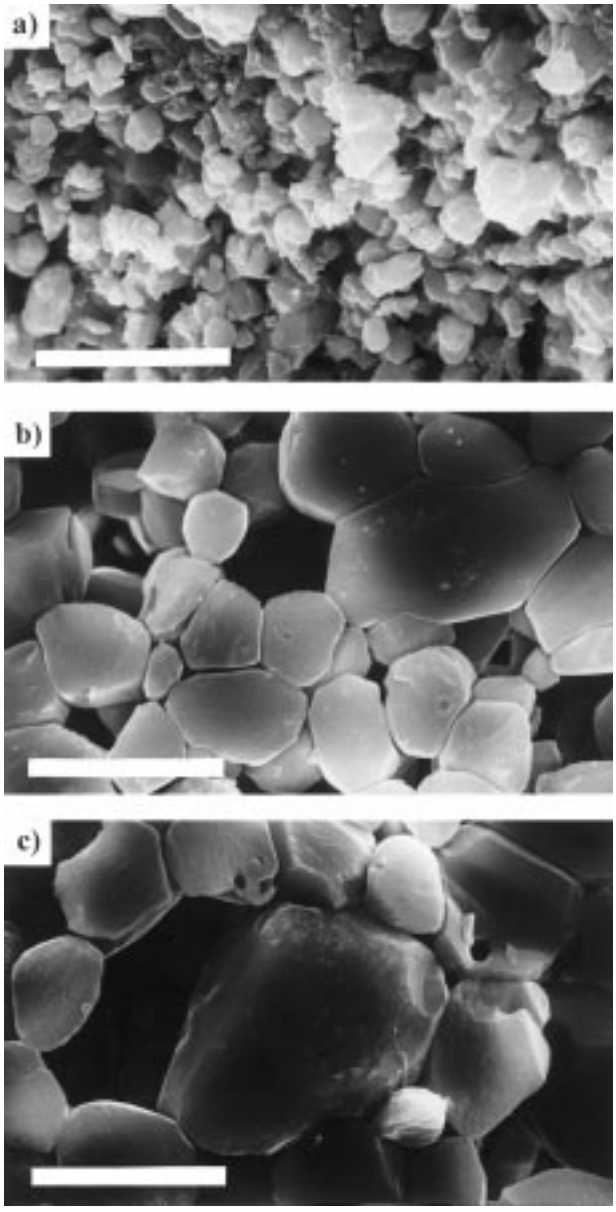

Fig. 2. SEM micrographs of HA sintered with Li^+: (a) sample A; (b) sample B; (c) sample C. Bar = 10 μm.

With the aim of relating the properties of the material to its composition and structure, dissipation factor (D) and dielectric constant (K) measurements were made. In particular, dissipation factor in dielectric ceramic materials results from two simultaneous processes: (a) dc–conductivity losses at low frequencies; (b) losses due to ion jumps and dipole relaxations [7]. In Fig. 4 the dissipation factor is plotted as a function of frequency for the samples with Li^+. It can be seen that, as previously expressed, at low frequencies the main cause contributing to dissipation factor is the dc-conductivity loss. The same trend was observed for dc-conductivity curves. An increase in these properties was detected from B to A to C at low frequencies. To explain this behaviour, it is necessary to consider that the dissipation mechanism in HA is due to OH^- jumps [11], and also to the presence of oxygen vacancies in β-TCP [10]. In this way, the decrease of the dissipation factor in sample B could be justified by the lower content of crystalline β-TCP. On the other hand, the sequence of the obtained values for

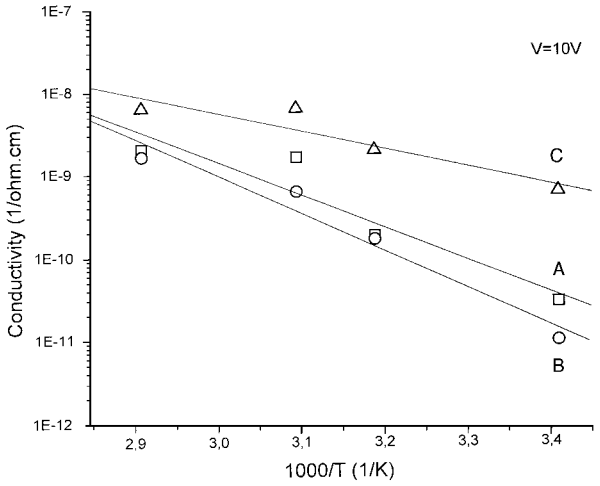

Fig. 3. DC-conductivity vs $1000/T$ for samples A, B, C.

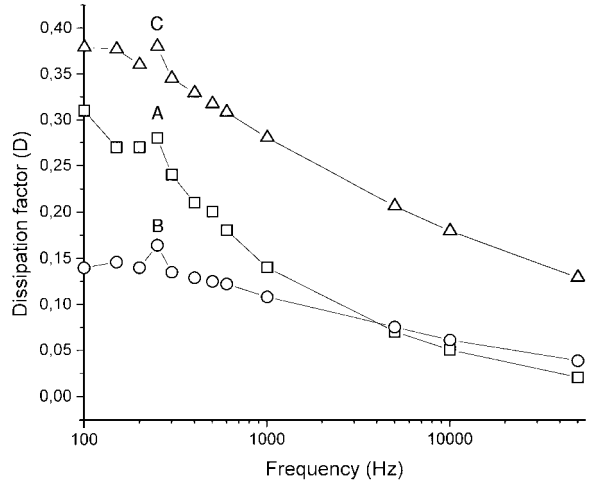

Fig. 4. Dissipation factor (D) vs frequency for samples A, B, C.

the dissipation factor is altered for frequencies higher than 10 kHz in samples A and B. This could be due to a new contribution to dissipation factor, from the relaxation of Li^+-vacancy dipoles inside the vitreous phase. However, for sample C the dissipation factor is always higher; this might be attributed to a greater contribution to the dissipation factor of Li^+-vacancy dipoles inside the vitreous phase.

Table 3 lists the results of the microhardness measurements in Li^+-containing samples. The maximum in microhardness occurs when the Li^+ content is 0.2%. This could be explained through the increase in density of the material; however, as the Li^+ content increases, the microhardness should be approximately constant and similar to that of sample B. This means that the porosity of C is not the cause of its lower microhardness. Instead, this may be attributed to the vitreous phase contained in the sample with 0.4% Li^+. These results agree well with the measurements of dc-conductivity versus 1/T previously discussed.

In Fig. 5, the SEM micrographs of the samples with Mg^{2+} are shown. In sample D, agglomerates of free MgO were observed, and identified by EPMA. XRD analyses of samples A, D, E and F showed that the angular position of the β-TCP peak at $d = 2.87$ Å slightly shifts (Table 4), suggesting that a significant part of the added Mg^{2+} ions is incorporated to the crystal structure of the phosphate, resulting in a diminution of the unit cell size. At the same time, the cell parameters of HA did not show variations, indicating that under the experimental conditions used, there is no detectable dissolution of Mg^{2+} in HA. Furthermore, as seen in Fig. 1, in these samples the presence of free low-crystallinity MgO was observed.

The values of dielectric constant (K) and of total porosity of the samples containing Mg^{2+} are given in Table 5. From these data, it can be seen that the dielectric constant of these materials varies inversely with the percent porosity. In samples E and F, a lowering of the dielectric constant is observed, due to the effect of the porosity of the samples and to the presence of MgO particles (the dielectric constant of MgO is 8.2 at 1 MHz [12]). This latter effect becomes more important at higher Mg^{2+} contents.

Table 3
Microhardness measurements of the samples

Sample	Microhardness (GPa)
A	4.6
B	5.9
C	4.6
D	4.2
E	2.4
F	2.7

Table 4
β-TCP peak position and interplanar spacing for sample with Mg^{2+}

Sample	°2θ	d(Å)
A	31.12	2.87
D	31.15	2.87
E	31.12	2.87
F	31.21	2.86

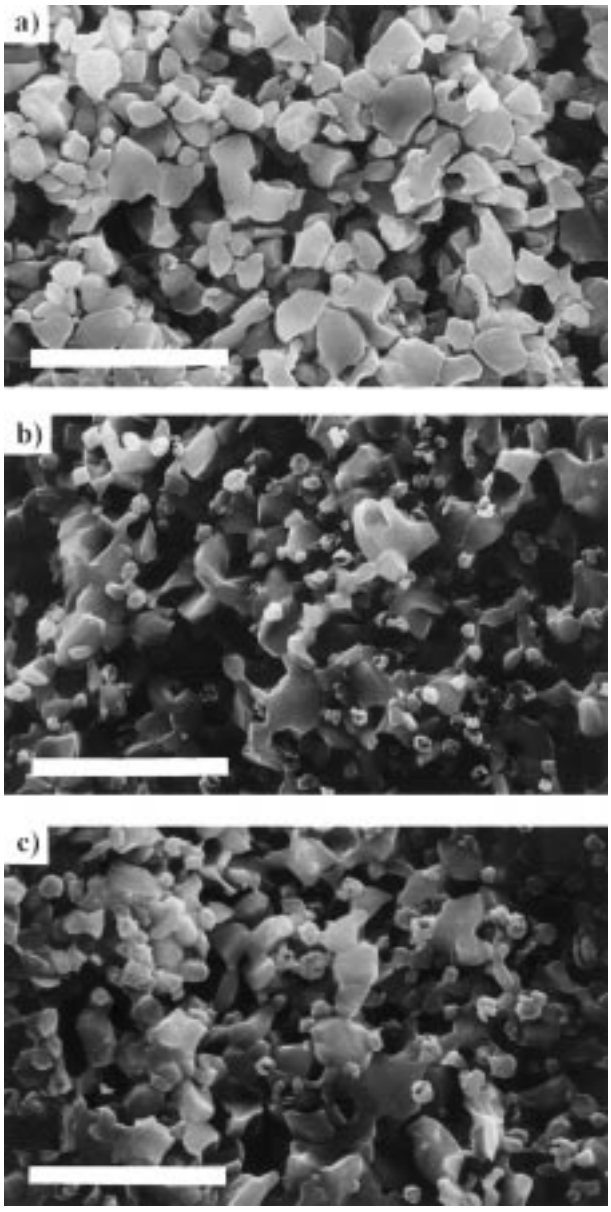

Fig. 5. SEM micrographs of HA sintered with Mg^{2+}:(a) sample D; (b) sample E; (c) sample F. Bar = 10 μm.

Table 5
Dielectric constant (K) at 1 MHz and porosity of samples with Mg^{2+}

Sample	K	Porosity %
A	12.61	14
D	13.62	11
E	9.81	16
F	9.45	17

From the dc-conductivity vs time curves (Fig. 6) for the samples A, D, E, F, it is possible to determine that Mg^{2+} additions produce a decrease in conductivity. The curves correspond to measurements at room temperature, but the same trend was observed along the entire temperature range studied (20–400°C). This behaviour is explained taking into account: the increment in porosity in samples E and F; the decrease in β-TCP concentration (which has a conductivity higher than that of sample A); the fact that Mg^{2+} can distort the β-TCP structure, modifying the mobility of oxygen vacancies; and finally the presence of agglomerates of free MgO.

From dissipation factor (*D*) measurements obtained at different frequencies, a progressive decrease of *D* was observed for samples D and E, with respect to A (Fig. 7). At low frequencies, the variation in dissipation factor for samples A, D, E, corresponds with the obtained values of conductivity, showing that dc-conductivity losses are the most important in this range. On the contrary, at frequencies higher than 10 kHz, the values for samples A and D are reverted. To explain this change it is necessary to consider that Mg^{2+} is incorporated to the β-TCP structure, modifying the ionic environment. Sample F shows a dissipation factor greater than E; this may be due to the presence of MgO particles. These induce a strong absorption at low frequencies, as well as polarizability changes, justifying the shift of the dissipation factor peak, and the higher losses with respect to sample E [13].

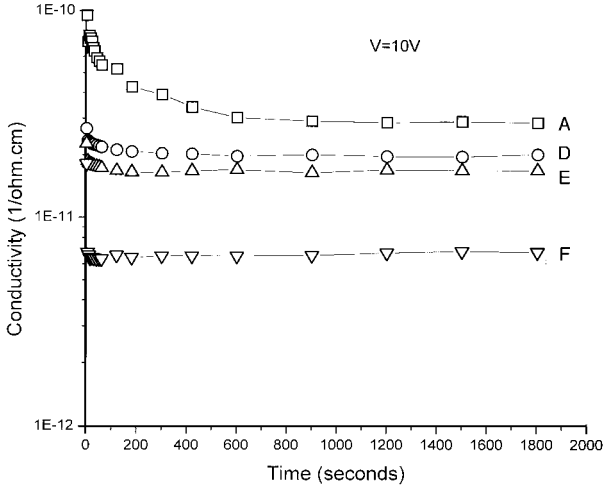

Fig. 6. DC-conductivity vs time for samples A, D, E, F.

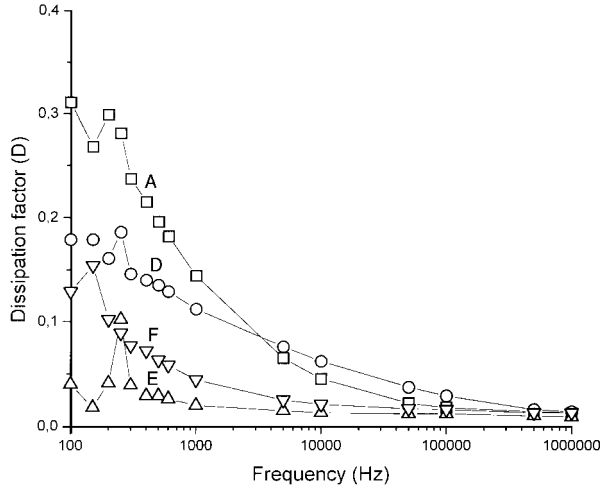

Fig. 7. : Dissipation factor (*D*) vs frequency for samples A, D, E, F.

Table 3 shows the microhardness determined for sintered samples with Mg^{2+}. The variation in microhardness is significative when passing from 1 to 3% Mg^{2+}. This difference is not justifiable by the variation in porosity alone, but also microstructural aspects must be considered. A quantitative analysis by XRD showed that the β-TCP content is lower in the samples with Mg^{2+}, with respect to sample A, remaining almost constant (approx. 10%) for all Mg^{2+} contents. Furthermore, XRD analyses showed that in samples E and F the free MgO content is about 4 times higher than in sample D; also, the MgO present in these samples is not highly crystalline, because it is formed by decomposition of magnesium nitrate during the thermal treatment. In Fig. 5(c) small particles of MgO with internal porosity are observed. For this reason, it must be kept in mind that the microhardness of these materials is affected by several factors (porosity, free MgO particles, variations in β-TCP content). The individual analysis of that factors suggests that free MgO content is the one which has the highest effect in microhardness.

4. Conclusions

Through the electrical and microstructural characterisation of non-stoichiometric HA ceramics sintered with additions of Li^+ or Mg^{2+}, it was determined that:

(a) The presence of 0.2% Li^+ in HA sintering causes a significant enhancement of densification, yielding materials with homogeneous microstructures. However, this is not accompanied by appreciable variations in electrical conductivity. Greater Li^+ additions result in higher vitreous phase contents, resulting in higher conductivities. An increase in vitreous phase content favours ionic mobility; at the same time, Li^+ ions become available carriers in the samples with 0.4% Li^+. The increase in dissipation factor in the sample with 0.4% lithium is mainly due to losses by dc-conductivity at low frequencies, and to the presence of Li^+-vacancy dipoles into the vitreous phase at high frequencies. The diminution of microhardness in samples with high Li^+ contents may be due to greater amounts of vitreous phase.

(b) HA sintered with Mg^{2+} shows higher densification only with 1% Mg^{2+}. For higher Mg^{2+} contents, densities and microstructures are affected by the formation of MgO aggregates, which also produce a significative decrease in the dielectric constant. The lower conductivity of the samples may be attributed to the higher porosity, the lowering of β-TCP content, and the presence of free MgO particles. These particles produce changes in the polarizability of the samples, resulting in a shifting of the peak, and in an increase in the dissipation factor. The marked decrease in microhardness of the samples with high Mg contents is produced by MgO agglomerates of low crystallinity.

From these results it is possible to establish that an addition of 0.2% of lithium or 1% of magnesium improves the microstructure and the microhardness of the samples. Greater lithium or magnesium additions produce higher vitreous phase contents or more MgO agglomerates, respectively, resulting in a diminution in the microhardness.

References

[1] H. Aoki, Medical Applications of Hydroxyapatite. Ishiyaku EuroAmerica, Tokyo, 1994.
[2] M.A. Fanovich, J.M. Porto Lopez, Influence of temperature and additives on the microstructure and sintering behavior of hydroxyapatites with different Ca/P ratio. J. Mater. Sci.: Mater. in Medicine, 9 (1998) 53–60.
[3] T. Goto, N. Wakamatsu, H. Kamemizu, M. Iijima, Y. Moriwaki, Sintering mechanism of hydroxyapatite by addition of lithium phosphate, J. Mat. Sci. 26 (1991) 1149–1152.
[4] E. Ochiai, in: S.A. Reverté (Ed.), Bioinorganic Chemistry, Barcelona, 1985.
[5] E.J. Baran, in: Fava (Ed.), Química Bio-Inorgnica, La Plata, Argentina, 1984, p. 91.
[6] M. Okazaki, Crystallographic behavior of fluoridated hydroxyapatites containing Mg^{+2} and CO_3^{-2} ions, Biomaterials 12 (1991) 831–835.
[7] W.D. Kingery, H.K. Bowen, D.R. Uhlmann, Introduction to Ceramics. John Wiley & Sons, New York, 1975, pp. 847–974.
[8] P. Gu, J.J. Beaudoin, Dielectric behavior of hardened cement paste systems, J. Mater. Sci. Lett. 15 (1996) 182–184.
[9] K Yamashita, K. Kitagari, T. Umegaki, Thermal instability and proton conductivity of ceramic hydroxyapatite at high temperatures, J. Am. Ceram. Soc. 78 (5) (1995) 1191–1197.
[10] M.A. Fanovich, M.S. Castro, J.M. Porto Lopez, Improvement of the microstructure and microhardness of hydroxyapatite ceramics by addition of lithium. Mater. Lett. 33 (1998) 269–272.
[11] J.J. Prieto Valdéz, A. Victorero Rodríguez, J. Guevara Carrio, Dielectric properties and structure of hydroxyapatite ceramics sintered by different condictions, J. Mater. Res. 10 (9) (1995) 2174–77.
[12] R.C. Buchanan (Ed.), Properties of ceramic insulators, in: Ceramic Materials for Electronics, Marcel Dekker, New York, 1986, pp. 1–77C.
[13] R. Moreno, P. Miranzo, J. Requena, J. S. Moya, Effect of power characteristics on dielectric properties of alumina compacts, in: Ceramic Transactions Vol. 21, The American Ceramic Society, Ohio, 1991, pp. 225–233.